Localizing gene regulation reveals a staggered wood decay mechanism for the brown rot fungus *Postia placenta*

Jiwei Zhang[a], Gerald N. Presley[a], Kenneth E. Hammel[b,c], Jae-San Ryu[d], Jon R. Menke[e], Melania Figueroa[f], Dehong Hu[g], Galya Orr[g], and Jonathan S. Schilling[a,1]

[a]Department of Bioproducts and Biosystems Engineering, University of Minnesota, Saint Paul, MN 55108; [b]Institute for Microbial and Biochemical Technology, US Forest Products Laboratory, Madison, WI 53726; [c]Department of Bacteriology, University of Wisconsin, Madison, WI 53706; [d]Eco-Friendliness Research Department, Gyeongsangnam-do Agricultural Research and Extension Services, Jinju 660-360, Republic of Korea; [e]Department of Plant Biology, University of Minnesota, Saint Paul, MN 55108; [f]Department of Plant Pathology, University of Minnesota, Saint Paul, MN 55108; and [g]Chemical and Biological Sciences Divisions, Pacific Northwest National Laboratory, Richland, WA 99354

Edited by Caroline S. Harwood, University of Washington, Seattle, WA, and approved July 29, 2016 (received for review May 26, 2016)

Wood-degrading brown rot fungi are essential recyclers of plant biomass in forest ecosystems. Their efficient cellulolytic systems, which have potential biotechnological applications, apparently depend on a combination of two mechanisms: lignocellulose oxidation (LOX) by reactive oxygen species (ROS) and polysaccharide hydrolysis by a limited set of glycoside hydrolases (GHs). Given that ROS are strongly oxidizing and nonselective, these two steps are likely segregated. A common hypothesis has been that brown rot fungi use a concentration gradient of chelated metal ions to confine ROS generation inside wood cell walls before enzymes can infiltrate. We examined an alternative: that LOX components involved in ROS production are differentially expressed by brown rot fungi ahead of GH components. We used spatial mapping to resolve a temporal sequence in *Postia placenta*, sectioning thin wood wafers colonized directionally. Among sections, we measured gene expression by whole-transcriptome shotgun sequencing (RNA-seq) and assayed relevant enzyme activities. We found a marked pattern of LOX up-regulation in a narrow (5-mm, 48-h) zone at the hyphal front, which included many genes likely involved in ROS generation. Up-regulation of GH5 endoglucanases and many other GHs clearly occurred later, behind the hyphal front, with the notable exceptions of two likely expansins and a GH28 pectinase. Our results support a staggered mechanism for brown rot that is controlled by differential expression rather than microenvironmental gradients. This mechanism likely results in an oxidative pretreatment of lignocellulose, possibly facilitated by expansin- and pectinase-assisted cell wall swelling, before cellulases and hemicellulases are deployed for polysaccharide depolymerization.

biodegradation | bioconversion | decomposition | lignocellulose | cellulase

Brown rot wood-degrading fungi release sequestered carbon from lignocellulose in forests (1) and have the unique ability to accomplish this without significantly removing the recalcitrant lignin that encases the structural polysaccharides. Accordingly, their decay mechanisms may provide a model for new biomass conversion technologies that not only function despite the presence of lignin but also yield lignin as a potentially useful coproduct (1–3). Deviating from their white rot ancestors, brown rot fungi have evolved mechanisms that are generally faster (4, 5) and more polysaccharide-specific because they circumvent lignin (4, 6–8). This enhanced efficiency is coupled with losses, not expansions, of key white rot genes, including many linked to lignin degradation and processive cellulose hydrolysis. For example, few brown rot fungi produce the cellobiohydrolases that are included in commercial synergistic glycoside hydrolase (GH) mixtures (9–12). These observations imply that brown rot fungi harbor novel pathways to improve saccharification yields.

To explain why brown rot fungi are so efficient, despite their minimal toolkit of biodegradative enzymes, low-molecular-weight (LMW) oxidative agents have been proposed to operate in tandem with the enzymes. There is considerable evidence that extracellular Fenton reactions play a key role during brown rot, producing highly oxidizing hydroxyl radicals ($H_2O_2 + Fe^{2+} \rightarrow OH^- + Fe^{3+} + \bullet OH$) or similarly reactive iron–oxo complexes. These oxidants apparently modify the lignocellulose to make it more susceptible to enzymatic saccharification by the limited set of GHs that brown rot fungi have retained in their genomes (13–18). In agreement, modifications in the lignin of brown-rotted wood indicate that limited oxidative cleavage of the polymer has occurred (19–21).

It is debated, however, how brown rot fungi direct Fenton reagents, which exhibit negligible selectivity for targets, to react with lignocellulose without damaging fungal hyphae or extracellular GHs. A long-standing hypothesis proposes that the fungi produce microenvironmental gradients that spatially partition the oxidants from the GHs in wood cells. A common model has Fe^{3+} at low pH (<3) in the vicinity of the hyphae strongly chelated by secreted oxalate, hindering its reduction to the Fe^{2+} required for Fenton chemistry. Diffusion of these chelates into a higher pH (>5) wood cell wall, where GHs cannot penetrate and the oxalate concentration

Significance

Wood-decomposing fungi are key players in the carbon cycle and are models for making energy from lignocellulose, sustainably. Our study focuses on brown rot fungi that selectively remove carbohydrates, leaving most lignin behind. These fungi often decompose wood faster than their lignin-degrading white rot ancestors, despite losses in genes involved in plant cell wall hydrolysis. To explain brown rot, many have implicated reactive oxygen species (ROS) in facilitating hydrolysis, with microenvironmental gradients partitioning ROS from enzymes. By spatially colocalizing gene expression and enzyme activities as *Postia placenta* colonizes wood, we provide evidence of an oxidative-hydrolytic two-step mechanism controlled by differential expression, not microenvironments, and we highlight 549 genes (~4% of the genome) that are upregulated during this unique pretreatment.

Author contributions: J.Z., K.E.H., M.F., D.H., G.O., and J.S.S. designed research; J.Z., G.N.P., J.-S.R., J.R.M., D.H., G.O., and J.S.S. performed research; J.Z., G.N.P., K.E.H., M.F., and J.S.S. analyzed data; and J.Z., G.N.P., K.E.H., M.F., and J.S.S. wrote the paper.

The authors declare no conflict of interest.

This article is a PNAS Direct Submission.

Freely available online through the PNAS open access option.

Data deposition: The data reported in this paper have been deposited in the Gene Expression Omnibus (GEO) database, www.ncbi.nlm.nih.gov/geo (accession no. GSE84529).

[1]To whom correspondence should be addressed. Email: schillin@umn.edu.

This article contains supporting information online at www.pnas.org/lookup/suppl/doi:10.1073/pnas.1608454113/-/DCSupplemental.

is proposed to be lower, then results in their disassociation. With reactive Fe^{3+} thus available, LMW reductants secreted by the fungus could generate Fe^{2+} within the lignocellulose matrix and at a safe distance from hyphae and GHs (22).

Validating this hypothesis has proven difficult, and an underlying weakness lies in the high diffusivity of both H^+ ions and small metal ion chelates, which would limit significant concentration gradients between fungal hyphae and the wood cell wall (23). A more feasible way to separate an oxidative pretreatment from enzymatic saccharification would be via differential expression, and this staggered approach might have added benefit in withholding metabolically costly GHs until they can operate effectively. There is evidence that fungal methoxyhydroquinones with a role in reducing Fe^{3+} to initiate Fenton chemistry are mostly secreted at the outset of brown rot, and then decrease as decay progresses (7, 16, 24, 25). There is also evidence of inducible expression and secretion of enzymes among brown rot fungi (9, 26), once characterized as having constitutive cellulase production (27). However, it has so far not been possible to determine whether the oxidative and GH systems are temporally separated by these fungi on wood. A major impediment to progress has been the heterogeneous nature of fungal colonization and attack on wood, during which adjacent regions of the substrate are frequently at different stages of decay.

To address this problem, we elicited growth of the brown rot fungus *Postia placenta* in one direction along thin wood specimens. This approach spatially separated the stages of decay linearly along the substrate. We then sectioned the wood and analyzed individual sections for gene expression at the whole-transcriptome level, as well as enzyme activities they encode [defined here as lignocellulose oxidation (LOX) genes and GHs; *SI Materials and Methods*], with a particular focus on lignocellulolytic genes relevant to both oxidative and GH aspects of the brown rot mechanism. The reassembled data show temporal trends in expression, extending back from the advancing hyphal front, on a finer scale than is possible using conventional culture methods on wood. Our results reveal evidence that staggered gene expression has a role in regulating the progress of brown rot.

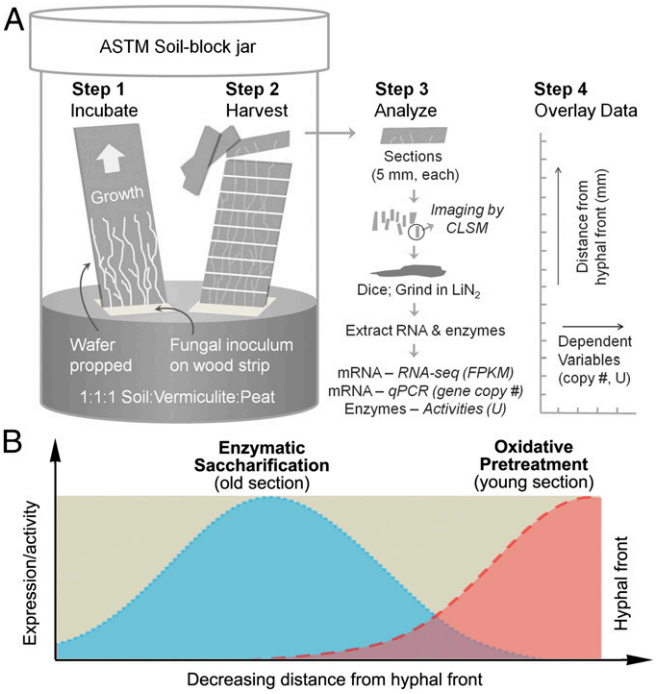

Fig. 1. Schematic of wafer setup and staggered mechanism hypothesis. (*A*) *P. placenta* was cultured in modified American Society for Testing and Materials (ASTM) soil-block microcosms, with wood wafers propped to force fungi to grow vertically. This setup generated a spatiotemporal gradient along the advancing mycelium, delineated by the visible advancing hyphal front and reconstructed from sections. LIN_2, liquid nitrogen. (*B*) Data from RNA-seq, quantitative PCR (qPCR), confocal laser scanning microscopy (CLSM), and enzymatic activity assays were layered (i.e., stacked) in specific zones relative to the hyphal front and used to test the hypothesis that brown rot fungi stagger the expression of genes and extracellular enzymes during wood decay.

Results

Wafer Colonization. Decay microcosms elicited directional growth by *P. placenta* on both aspen and spruce wood wafers, resulting in distinct fronts of advancing hyphae that could be sectioned spatially to reconstitute a well-resolved temporal sequence (Fig. S1*A*). Mycelial growth rates were ~2.5 $mm{\cdot}d^{-1}$; thus, the 0- to 5-mm sections used to represent early decay represented a *ca.* 48-h window. Confocal microscopy verified that the hyphal front within the wood matrix coincided with the visible front on the surface (methods are provided in *SI Materials and Methods*). Fungal biomass increased in the wood over time, with more branching near the wafer base in older hyphae, but with tips and branching evident in all wafer sections (Fig. S1*B*). Once colonization had extended ~50 mm up the 60-mm wafers, triplicate wafers with uniform hyphal fronts (horizontal and linear) were cut into sections to assess the hypothesis of a staggered oxidative-hydrolytic mechanism (Fig. 1), with the hyphal front assigned a position of 0 mm. Among these sections, preliminary quantitative PCR analysis done on colonized spruce wood showed staggered gene regulation patterns, with transcripts for six oxidoreductases relatively more abundant at the hyphal front and transcripts for eight (hemi)cellulases accumulating distally (Fig. S2).

Staggered Gene Expression During Brown Rot. Whole-transcriptome shotgun sequencing (RNA-seq) analysis showed differential expression of genes involved in substrate oxidation vs. polysaccharide hydrolysis, based on analyses of aspen wafer sections at three locations (0–5, 15–20, and 30–35 mm). The overall gene expression profiles were similar for older mycelium on the two sections at 15–20 and 30–35 mm, whereas they were clearly different for the younger mycelium at 0–5 mm (Fig. S3 and Dataset S1; Gene Expression Omnibus database accession no. GSE84529). Considering the 0- to 5-mm sections as representative of early decay and the two older sections together as representative of late decay, differentially expressed genes (DEGs) were screened for greater than fourfold changes in transcript accumulation [false discovery rate (FDR) < 0.05 and fragments per kilobase unique exon sequence per megabase of library mapped (FPKM) > 5; DEG definition is provided in *SI Materials and Methods*]. For brevity, we arbitrarily refer to genes meeting this criterion as "upregulated." In total, 549 DEGs were up-regulated during early decay, and sequences that encode oxidoreductase activities, such as incorporation or reduction of O_2 and heme/iron binding, were significantly enriched [FDR < 0.05 for Gene Ontology (GO) enrichment]. In contrast, 659 DEGs were up-regulated during late decay, and, among them, sequences that encode GH activities were significantly enriched (FDR < 0.05; Fig. S4 and Dataset S2).

Oxidoreduction-Associated Genes. RNA-seq analysis identified 33 genes up-regulated during early decay that are likely associated with redox processes, such as LOX. Of these genes, 21 (designated LOX_Fenton) may be involved in generating H_2O_2 or Fe^{2+} to support biodegradative Fenton chemistry (Fig. 2 and Table S1). These LOX_Fenton genes encode enzymes that putatively include glucose oxidases [protein IDs 44331 and 128830 from the Joint Genome Institute (JGI) database, *P. placenta* v1.0], alcohol oxidases (55972 and 129158/126217), glyoxal oxidase (46390), amino acid/amine oxidases (47008 and 110689), iron reductases (130025 and 130030/130043), and Fe^{2+} transporters (52765/43266). In addition, eight genes with likely roles in the biosynthesis of aromatic

MICROBIOLOGY

metabolites were up-regulated during early decay [e.g., benzoquinone reductases (124517/64069), phenylalanine ammonia lyase (111514), aromatic ring monooxygenases (54109/46071, 23052/62058, and 129128)]. The encoded enzymes may be involved in the biosynthesis of secreted methoxyhydroquinones, which drive extracellular Fenton chemistry by reducing Fe^{3+} to Fe^{2+} (7, 16, 24, 25). One O-methyltransferase (52307) putatively involved in methoxyhydroquinone synthesis was also up-regulated by about twofold ($P < 0.05$) (Dataset S1).

Also relevant to LOX was the up-regulation of 31 cytochrome P450s during early decay vs. six that were up-regulated during later decay (Fig. 2 and Dataset S3). Some cytochrome P450s are likely involved in aromatic hydroxylation reactions required for methoxyhydroquinone biosynthesis, as well as the hydroxylation of lignin fragments preparatory to aromatic ring fission (28).

With regard to Fe^{3+} mobilization, the expression of genes associated with production of the physiological iron chelator oxalate (16) followed a pattern that suggests stimulation followed by attenuation. On the production side, we found two putative glyoxylate dehydrogenase genes (121561/115965) and one putative oxaloacetate acetylhydrolase gene (112832) that were markedly up-regulated by more than 60-fold during early decay (Table S1). This was countered during later decay by an up-regulation of likely oxalate decarboxylases (46778 and 43912) at far higher expression levels than we found for another oxalate decarboxylase (61132) that was up-regulated near the hyphal front.

Among 21 oxidoreductases that were up-regulated during later decay, there were seven genes in the LOX_Fenton category, including two aryl alcohol oxidases, a ferroxidase, and a transmembrane iron permease; two iron reductases (127865/129444); and a glutathionyl-hydroquinone reductase (60536) (Table S1). Among the other LOX genes up-regulated during later decay, there were several that might be involved in detoxification rather than lignocellulose degradation, including catalases (59021 and 99098), superoxide dismutases (110493/111797), and a glutathione S-transferase (60536). Aromatic compound dioxygenases (119457/125432 and 34850) and a polysaccharide monooxygenase (115618/126811) were also up-regulated late rather than early, presumably to cleave lignin fragments and polysaccharides, respectively, during this stage of decay.

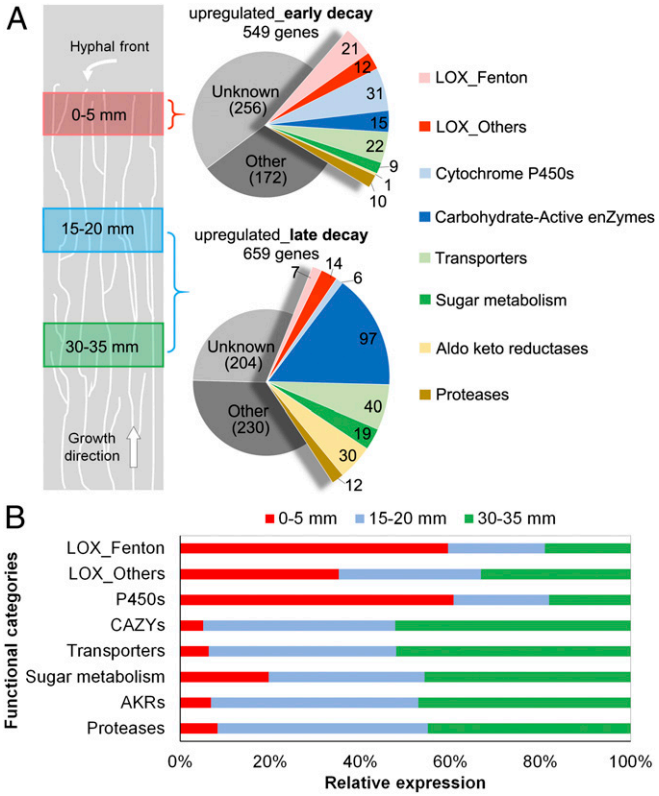

Fig. 2. Gene transcription patterns along the advancing hyphal front in aspen wafers as measured by RNA-seq. (*A*) Distribution of DEGs. Relative to sections at 15–20 mm and 30–35 mm, which represent late decay, 549 genes were up-regulated in sections at 0–5 mm, which represent early decay. Conversely, 659 genes were up-regulated during late decay. Data were obtained from three bioreplicates at each position. (*B*) Relative expression levels in different gene categories. The relative FPKM levels of DEGs in each category were compared among the sections of the three lengths. For DEGs, the fold change was >4 (FDR < 0.05) and the FPKM was >5. The LOX_Fenton category includes enzymes that may support extracellular Fenton chemistry (e.g., via extracellular H_2O_2 generation, iron reduction and homeostasis, hydroquinone biosynthesis, quinone redox cycling). LOX_Others includes genes that may be involved in lignin/aromatic compound modification, oxalate metabolism, polysaccharide monooxygenation, and protection from reactive oxygen species (9, 57). CAZy genes were assigned according to the CAZy database (www.cazy.org) (58). The assignment of other gene categories is provided in Dataset S3. AKR, aldo keto reductase.

Carbohydrate-Active Enzyme and Sugar Transporter Genes. A total of 97 carbohydrate-active enzyme (CAZy) genes involved in lignocellulose hydrolysis were up-regulated during later decay. This list includes 70 GHs (*P. placenta* has 255 predicted GH genes), 15 carbohydrate esterases, 6 glycosyl transferases, 3 feruloyl esterases, and 3 carbohydrate-binding module family genes (Fig. 2). Those differentially expressed CAZys that are likely involved in lignocellulose saccharification and have been predicted as secreted enzymes (50 total, 82% of them GHs) are listed in Table S2, including well-characterized endoglucanases Cel5A 115648/108962, Cel5B 103675/117690, and Cel12A 121191/112658, a xylanase (Xyn10A-1 113670/90657), and a mannanase (Man5A 57321/121831), as shown by previous work with *P. placenta* (9, 26, 29). Consistent with an increase in polysaccharide hydrolysis, sugar transporters, sugar-metabolic enzymes, and aldo keto reductases were also up-regulated during later decay stages (Dataset S3).

Some CAZys and relevant sugar transporters were up-regulated at the hyphal front relative to older hyphae (Table S2 and Dataset S3), including four GHs and two expansin-like genes. Notably, a polygalacturonase (111730/43189, pectinase) was up-regulated by about 15-fold during early decay, with a maximum FPKM approaching 1,800 at the hyphal front.

Enzyme Activities and Colocalization. Endoglucanase (carboxymethylcellulase)-, xylanase-, and mannanase-specific activities (units per milligram of fungal biomass) were low at the hyphal front and increased distally. Similar trends were shown for β-glucosidase, β-xylosidase, β-mannosidase, and α-arabinofuranosidase activities (Fig. 3*A*). In line with these results, Western blot analysis of one endoglucanase, Cel5B (103675/117690), showed that this protein was nearly undetectable at the hyphal front (0–5 mm) but substantially increased distally at 15–20 and 30–35 mm (Fig. 3*B*). The above results are in line with the RNA-seq results for Cel5B and other GH genes.

Among the LOX enzymes, relatively few are predicted to be secreted, but we were able to perform several assays. Catalase activity increased by nearly sixfold at 30–35 mm compared with the hyphal front (Fig. 3*A*), in line with the up-regulated expression patterns of catalase genes in older hyphae. For alcohol oxidase and glucose oxidase assays, no activities were detected, perhaps due to proteins being intracellular or periplasmic, or because the catalase activity may have consumed the H_2O_2 whose production is the basis for the oxidase assays. We also assayed laccase activities, and although these activity levels were low, colorimetric observations of 2,2′-azino-bis(3-ethylbenzothiazoline-6-sulfonic acid) (ABTS) oxidation in the extracts revealed a gradient opposite to the gradient of the GH activities, with the highest activity

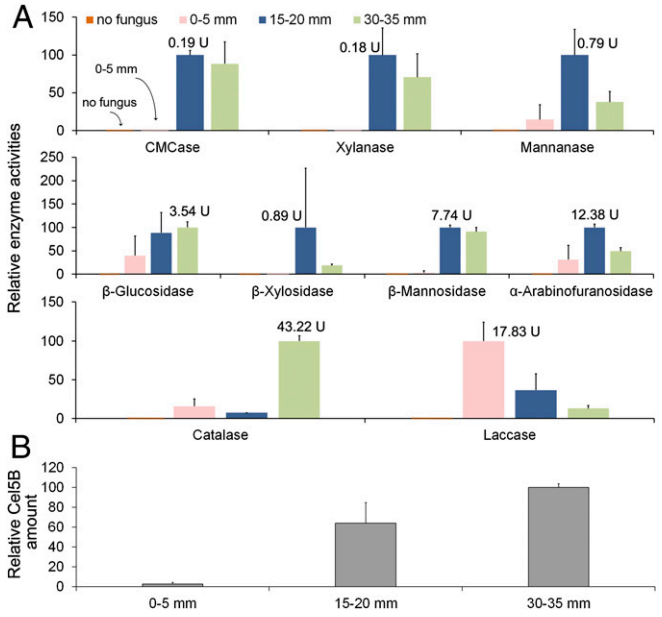

Fig. 3. Presence and activity of *P. placenta* GHs and oxidoreductases in aspen wafers. (*A*) Relative activities of relevant water-extracted enzymes with likely lignocellulolytic roles (*SI Materials and Methods*). Activities were measured as units per milligram of total fungal protein and were normalized for each enzyme by setting the highest activity (shown beside the column) at 100. (*B*) Relative amounts of secreted endoglucanase Cel5B (protein ID 103675/117690) via Western blotting. Error bars represent the SD of two bioreplicates, with 12 wafers' sections pooled for each replicate.

located at the hyphal front. This result is in line with the RNA-seq results for one candidate laccase (47589), which was up-regulated by 1.8-fold at the hyphal front ($P < 0.05$) (Dataset S1).

Discussion

Our results support a two-step oxidative-hydrolytic mechanism for the brown rot fungus *P. placenta*, which entails a brief oxidative pretreatment that has been obscured in earlier studies. We arrived at this conclusion by growing the fungus directionally, thus extending over space the temporal progression of decay, after which we performed both transcript analyses and enzyme assays. The results of the two approaches (transcriptomics and enzyme assays) agree with each other. The shift from oxidoreductase-dominated to GH-dominated expression by *P. placenta* generally occurred at a short distance behind the hyphal front, confining key oxidative dynamics to a narrow zone of mycelial growth. As an example, all three of *P. placenta*'s endoglucanases (Cel5A, Cel5B, and Cel12A) were up-regulated in the 15- to 20-mm aspen sections by 14-, 25-, and 26-fold, respectively, relative to values at the hyphal front (0- to 5-mm sections) (Table S2). By contrast, there was a reverse pattern in quinone reductase expression, as shown by a 10-fold decrease, in 15- to 20-mm sections vs. 0- to 5-mm sections (Table S1). In colonized spruce wood, for which immediately adjacent sections were analyzed at 5-mm intervals, quantitative PCR analysis showed that this interval of oxidoreductive gene up-regulation persisted for only 48 h, given the growth rates we observed (Fig. S2). This brief window of differential gene regulation has been missed in earlier studies of brown rot that used homogenized whole-wood specimens, likely because that approach inevitably mixes hyphae acting asynchronously at different stages of biodegradation (7, 9, 21, 26, 29).

Given that we observed both hyphal tips and branching hyphae in all wood sections yet were able to discern differential gene expression across the sections, our results raise the question of how uniformly *P. placenta* controls gene expression. A unified mechanism could apply locally to all cell types, but it is also possible that differential expression could be limited to a particular subpopulation of cells. Although apical hyphae are often presumed responsible for the bulk of fungal protein secretion (30, 31), expression patterns that are locally heterogeneous can arise due to nonuniform gene expression within the mycelium (32) and to protein secretion from subapical hyphal regions (33). Heterogeneous secretion of lignin peroxidases has, for example, been shown in the wood-degrading fungus *Phanerochaete chrysosporium* (34). In our case, we cannot discern the relative contributions of hyphal tips and subapical hyphae, but the well-defined gene up-regulation patterns we observed on a fine spatial scale are striking, given the heterogeneous hyphal populations.

Many of the up-regulated LOX genes in the frontal zone (0–5 mm) of the advancing *P. placenta* mycelium likely have roles in biodegradative Fenton chemistry (9, 35, 36). These processes include oxalate production for iron chelation, production of methoxyhydroquinones that reduce Fe^{3+} and O_2, enzymatic iron transport and reduction, and enzymatic H_2O_2 generation (Table S1). Some of these and other up-regulated LOX genes near the hyphal front of *P. placenta* have been classified as encoding auxiliary enzymes that support lignin degradation by white rot fungi (25). This category includes genes for the quinone reductase and the Δ^{12} fatty acid desaturase, both highly up-regulated in our case. The latter enzyme is linked to linoleic acid production and lignin degradation via lipid peroxidation in white rot fungi such as *Ceriporiopsis subvermispora* (37, 38). Accordingly, it is possible that the functions of some up-regulated LOX genes in *P. placenta* have been adapted from white rot ancestors to enable a staggered oxidative-hydrolytic mechanism during brown rot. Retention or recruitment of some white rot LOX genes could contribute to the partial ligninolysis that brown rot fungi are able to achieve and could facilitate subsequent access by GHs that hydrolyze structural polysaccharides (19, 20, 39).

In distal sections of the *P. placenta* mycelium, the delayed and marked up-regulation of CAZys, specifically GHs, implies that cellulases and hemicellulases have a significant role in wood decay, contrary to the classical view that these enzymes cannot infiltrate the wood cell wall during brown rot (40). These CAZys include not only several previously characterized endoglucanases (29) but also numerous hemicellulases and carbohydrate esterases, many of which remain poorly characterized (e.g., feruloyl esterases, GH53 arabinogalactan endo-β-galactosidase). Some of these enzymes may be responsible for the early losses in hemicellulose side chains that characterize brown rot (41). Our observation of increased gene transcription and enzyme activity for α-L-arabinofuranosidase behind the hyphal front offers a representative example. This α-L-arabinofuranosidase is an enzyme within a family (GH43) that contains a great deal of subtle variation, not fully captured by assays that use simple synthetic substrates (42). These GH43s are expanded in many wood-degrading fungi, including *Schizophyllum commune* (43). Up-regulation of hemicellulases and carbohydrate esterases implies that enzymatic hemicellulose hydrolysis is integral to brown rot, even though hemicellulase genes [including GH43s (44)] are less numerous and less diverse in brown rot fungi than in white rot fungi (11).

The LOX genes up-regulated late, alongside the general up-regulation of GHs, include genes that may have a protective role rather than a direct role in lignocellulose deconstruction. For example, those genes encoding catalases may have a role in attenuating Fenton chemistry to prevent oxidative damage to GHs that are secreted during the hydrolytic stage of biodegradation (Table S1). In addition, aryl alcohol oxidases and glutathione S-transferases may be expressed as a detoxification response after oxidative pretreatments release potentially toxic fragments from lignocellulose (45, 46). This result also suggests that aryl alcohol oxidases, which are thought to participate in H_2O_2 generation to support lignin degradation by white rot fungi (47, 48), may have a different

function during brown rot, relegating H_2O_2 generation to another pathway.

Conversely, the CAZys up-regulated early, where LOX up-regulation dominated, may synergize with LOXs during decay initiation. These CAZys include a GH28 pectinase and two expansin-like proteins (Table S2). Expansins have been implicated in binding and swelling cellulose to improve accessibility (49), and expansin-like genes have been reported in the white rot fungus *Bjerkandrea adusta* (termed "loosenin") (50) and in *S. commune* (43). Their contribution might be complemented by the GH28 polygalacturonase (pectin depolymerase) of *P. placenta* (39% identity to the GH28 polygalacturonase in *Aspergillus niger*; GenBank database accession no. CAA38085.1), which may target pectin as an accessible, easily hydrolyzed polymer to uncouple lignocellulosic constituents as decay is initiated. This complementary coordination of gene regulation may also involve genes of unknown function, particularly when gene products include secretion signal peptides. These potential early roles for selected CAZys are also complicated by the fact that the proteins would be susceptible to damage by the extracellular reactive oxygen species-generating system, so additional work focused on these CAZys is in order. However, it is notable that synergy between polygalacturonases and oxalic acid is harnessed by bacteria to degrade plant cell walls (e.g., ref. 51), and was proposed by Green et al. (52) to initiate loosening of plant cell walls and facilitate access by brown rot fungi.

The expression patterns we report here support a two-step biodegradative mechanism in *P. placenta*, and may explain why brown rot is so efficient despite losses of many lignocellulolytic genes. Some of the components involved may show promise in biotechnological or other applied uses. Our results also underscore that it is important to consider how biodegradative components may be spatially segregated during the deconstruction of a complex, recalcitrant, solid substrate such as lignocellulose. The spatially resolved system we used here helps address this problem, and may offer a way to colocalize fungal expression patterns with physical modifications in wood (e.g., increases in porosity) that enable secreted proteins to access their substrates.

Materials and Methods

Colonization of Wood Wafers with *P. placenta*. *P. placenta* dikaryotic strain MAD 698-R (American Type Culture Collection 44394) was maintained on 1.5% (wt/vol) malt extract agar for routine culturing and to inoculate modified American Society for Testing and Materials soil-block microcosms (5). Vertically oriented wood wafers were colonized directionally from a predeveloped *P. placenta* hyphal mat. At harvest, wafers were sectioned to segregate the temporal progression of wood decay spatially, an approach modified from Schilling et al. (53) (Fig. 1*A*). In brief, a 1:1:1 mixture of soil, peat, and vermiculite hydrated to 40–45% (wt/vol) moisture content was packed into pint glass jars to one-third full. Feeder strips on the media surface were inoculated with 1-cm diameter agar plugs from *P. placenta* cultures and allowed to form a confluent mycelial lawn over 2–3 wk. Wood wafers were cut into 60 × 25 × 2.5-mm sections, with the largest face being the cross-section and with the tangential plane in contact with the mycelium when propped in jars. Cultures were incubated at room temperature for 3–4 wk until the visible hyphal front had advanced ∼50 mm up the wafers. Wafers with flat hyphal fronts (horizontal lines) were then harvested, scraped free of surface hyphae, and sectioned into 5-mm sections using a razor blade sterilized with each cut, with the first cut along the hyphal front. Distance from the hyphal front was used to delineate sections on wafers (Fig. 1*A*) for analyses per section in triplicate.

RNA Isolation and RNA-Seq Analysis. Total RNA for *P. placenta* was isolated from each wood section with TRIzol (Life Technologies) and then cleaned up with a Qiagen RNeasy Mini Kit (Qiagen, Inc.) to remove organic inhibitors before downstream RNA-seq or quantitative RT-PCR (qRT-PCR). For RNA-seq, TruSeq RNA v2 libraries were prepared and sequenced on a HiSeq 2500 System (Illumina, Inc.) by using the standard protocols from Illumina. Sequenced reads were mapped against the genome of *P. placenta* MAD 698-R (v1.0) with Tophat (v2.0.13) in the Galaxy platform (Table S3). By using the reference transcript models in the JGI database, expression levels (FPKM) and significances of differences were estimated with Cuffdiff (Galaxy Tool Version 2.2.1.3) using geometric normalization. The FDR was set as <0.05. The profiling data for whole-genome transcripts and DEGs are available in Dataset S1. Hierarchical clustering and GO enrichment of the DEGs were analyzed by HCE (v3.0) and Blast2Go (v3.2.7), respectively.

The expression levels of relevant LOX and GH genes were also analyzed via qRT-PCR along the advancing hyphal front in spruce wafers ($n = 3$) (Table S4). More detail is available in *SI Materials and Methods* about RNA extraction, RNA-seq, and qRT-PCR.

Protein Extraction, Enzyme Activity Assays, and Western Blotting. Sections at set distances from the hyphal front were pooled from wafers for protein extraction in 0.05 M citrate buffer (pH 5.0) for 24 h with stirring at 4 °C. The extracts were filtered through miracloth and 0.2-μm filters, and protein concentration was then determined using the Bio-Rad Protein Assay Kit (Bio-Rad). Activities of endoglucanase, xylanase, and mannanase were measured with dinitrosalicylic acid reagent using, respectively, three model substrates: 0.5% carboxymethyl cellulose, 0.5% birchwood xylan, and 0.25% locust bean gum (glucomannan), according to Ghose (54). β-Glucosidase, β-xylosidase, β-mannosidase, and β-arabinofuranosidase activities were measured by using 10 mM 4-nitrophenyl-β-D-glucopyranoside, 5 mM 4-nitrophenyl-β-D-xylopyranoside, 10 mM 4-nitrophenyl-β-D-mannopyranoside, and 1 mg·mL^{-1} 4-nitrophenyl-α-L-arabinofuranoside, respectively. Laccase activities of the crude extracts were measured with 0.5 mM ABTS as substrate (55). According to Aro et al. (56), fungal biomass in wood wafers was approximated by determining the 0.05 M NaOH-extractable proteins in different sections that had been ground in liquid N_2. The physical presence of endoglucanase Cel5B, a well-characterized GH of *P. placenta*, was also measured in the protein extracts using Western blotting (details are provided in *SI Materials and Methods*).

ACKNOWLEDGMENTS. This work was supported by the US Department of Energy Office of Science [Early Career Grant DE-SC0004012 from the Office of Biological and Ecological Research (BER) to J.S.S.; BER Grant DE-SC0012742 to J.S.S., K.E.H., M.F., and J.Z.]. Confocal microscopy was funded by User Facility Grant 48607 at the Environmental Molecular Sciences Laboratory of Pacific Northwest National Laboratory (to J.S.S., J.Z., and G.N.P.).

1. Mester T, Varela E, Tien M (2004) Wood degradation by brown-rot and white-rot fungi. *The Mycota II, Genetics and Biotechnology* (Springer-Verlag Berlin Heidelberg, New York), ed Kück U, 2nd Ed, pp 355–368.
2. Goodell B, Qian Y, Jellison J (2008) Fungal decay of wood: Soft rot-brown rot-white rot. *Development of Commercial Wood Preservatives*, ACS Symposium Series, eds Schultz T, et al. (American Chemical Society, Washington, DC), pp 9–31.
3. Schilling JS, et al. (2012) Lignocellulose modifications by brown rot fungi and their effects, as pretreatments, on cellulolysis. *Bioresour Technol* 116:147–154.
4. Cowling EB (1961) *Comparative Biochemistry of the Decay of Sweetgum Sapwood by White-Rot and Brown-Rot Fungi*, Technical Bulletin No 1258 (US Department of Agriculture, Washington, DC).
5. ASTM International (2007) *ASTM Standard D1413-07e1. Standard Test Method for Wood Preservatives by Laboratory Soil-Block Cultures* (ASTM International, West Conshohocken, PA).
6. Kleman-Leyer K, Agosin E, Conner AH, Kirk TK (1992) Changes in the molecular size distribution of cellulose during attack by white-rot and brown-rot fungi. *Appl Environ Microbiol* 58(4):1266–1270.
7. Suzuki MR, Hunt CG, Houtman CJ, Dalebroux ZD, Hammel KE (2006) Fungal hydroquinones contribute to brown rot of wood. *Environ Microbiol* 8(12):2214–2223.
8. Schilling JS, Kaffenberger JT, Liew FJ, Song Z (2015) Signature wood modifications reveal decomposer community history. *PLoS One* 10(3):e0120679.
9. Martinez D, et al. (2009) Genome, transcriptome, and secretome analysis of wood decay fungus *Postia placenta* supports unique mechanisms of lignocellulose conversion. *Proc Natl Acad Sci USA* 106(6):1954–1959.
10. Floudas D, et al. (2012) The Paleozoic origin of enzymatic lignin decomposition reconstructed from 31 fungal genomes. *Science* 336(6089):1715–1719.
11. Hori C, et al. (2013) Genomewide analysis of polysaccharides degrading enzymes in 11 white- and brown-rot Polyporales provides insight into mechanisms of wood decay. *Mycologia* 105(6):1412–1427.
12. Riley R, et al. (2014) Extensive sampling of basidiomycete genomes demonstrates inadequacy of the white-rot/brown-rot paradigm for wood decay fungi. *Proc Natl Acad Sci USA* 111(27):9923–9928.
13. Hammel KE, Kapich AN, Jensen KA, Ryan ZC (2002) Reactive oxygen species as agents of wood decay by fungi. *Enzyme Microb Technol* 30(4):446–453.
14. Koenigs JW (1974) Hydrogen peroxide and iron: A proposed system for decomposition of wood by brown-rot basidiomycetes. *Wood Fiber* 6(1):66–79.
15. Kerem Z, Bao W, Hammel KE (1998) Rapid polyether cleavage via extracellular one-electron oxidation by a brown-rot basidiomycete. *Proc Natl Acad Sci USA* 95(18):10373–10377.
16. Jensen KA, Jr, Houtman CJ, Ryan ZC, Hammel KE (2001) Pathways for extracellular Fenton chemistry in the brown rot basidiomycete *Gloeophyllum trabeum*. *Appl Environ Microbiol* 67(6):2705–2711.

17. Kramer C, Kreisel G, Fahr K, Kässbohrer J, Schlosser D (2004) Degradation of 2-fluorophenol by the brown-rot fungus Gloeophyllum striatum: Evidence for the involvement of extracellular Fenton chemistry. *Appl Microbiol Biotechnol* 64(3):387–395.
18. Rätto M, Ritschkoff AC, Viikari L (1997) The effect of oxidative pretreatment on cellulose degradation by *Poria placenta* and *Trichoderma reesei* cellulases. *Appl Microbiol Biotechnol* 48(1):53–57.
19. Filley TR, et al. (2002) Lignin demethylation and polysaccharide decomposition in spruce sapwood degraded by brown-rot fungi. *Org Geochem* 33(2):111–124.
20. Yelle DJ, Wei D, Ralph J, Hammel KE (2011) Multidimensional NMR analysis reveals truncated lignin structures in wood decayed by the brown rot basidiomycete *Postia placenta*. *Environ Microbiol* 13(4):1091–1100.
21. Kaffenberger JT, Schilling JS (2015) Comparing lignocellulose physiochemistry after decomposition by brown rot fungi with distinct evolutionary origins. *Environ Microbiol* 17(12):4885–4897.
22. Hyde SM, Wood PM (1997) A mechanism for production of hydroxyl radicals by the brown-rot fungus *Coniophora puteana*: Fe(III) reduction by cellobiose dehydrogenase and Fe(II) oxidation at a distance from the hyphae. *Microbiology* 143(1):259–266.
23. Hunt CG, et al. (2013) Spatial mapping of extracellular oxidant production by a white rot basidiomycete on wood reveals details of ligninolytic mechanism. *Environ Microbiol* 15(3):956–966.
24. Wei D, et al. (2010) Laccase and its role in production of extracellular reactive oxygen species during wood decay by the brown rot basidiomycete *Postia placenta*. *Appl Environ Microbiol* 76(7):2091–2097.
25. Korripally P, Timokhin VI, Houtman CJ, Mozuch MD, Hammel KE (2013) Evidence from *Serpula lacrymans* that 2,5-dimethoxyhydroquinone is a lignocellulolytic agent of divergent brown rot basidiomycetes. *Appl Environ Microbiol* 79(7):2377–2383.
26. Vanden Wymelenberg A, et al. (2010) Comparative transcriptome and secretome analysis of wood decay fungi *Postia placenta* and *Phanerochaete chrysosporium*. *Appl Environ Microbiol* 76(11):3599–3610.
27. Highley TL (1973) Influence of carbon source on cellulase activity of white-rot and brown-rot fungi. *Wood Fiber* 5(1):50–58.
28. Ide M, Ichinose H, Wariishi H (2012) Molecular identification and functional characterization of cytochrome P450 monooxygenases from the brown-rot basidiomycete *Postia placenta*. *Arch Microbiol* 194(4):243–253.
29. Ryu JS, et al. (2011) Proteomic and functional analysis of the cellulase system expressed by *Postia placenta* during brown rot of solid wood. *Appl Environ Microbiol* 77(22):7933–7941.
30. Wösten HAB, Moukha SM, Sietsma JH, Wessels JGH (1991) Localization of growth and secretion of proteins in *Aspergillus niger*. *J Gen Microbiol* 137(8):2017–2023.
31. Wessels JGH (1993) Wall growth, protein excretion, and morphogenesis in fungi. *New Phytol* 123(3):397–413.
32. de Bekker C, Bruning O, Jonker MJ, Breit TM, Wösten HA (2011) Single cell transcriptomics of neighboring hyphae of *Aspergillus niger*. *Genome Biol* 12(8):R71.
33. Hayakawa Y, Ishikawa E, Shoji JY, Nakano H, Kitamoto K (2011) Septum-directed secretion in the filamentous fungus Aspergillus oryzae. *Mol Microbiol* 81(1):40–55.
34. Moukha SM, Wösten HAB, Asther M, Wessels JG (1993) In situ localization of the secretion of lignin peroxidases in colonies of Phanerochaete chrysosporium using a sandwiched mode of culture. *J Gen Microbiol* 139(5):969–978.
35. Baldrian P, Valásková V (2008) Degradation of cellulose by basidiomycetous fungi. *FEMS Microbiol Rev* 32(3):501–521.
36. Korripally P, et al. (2015) Regulation of gene expression during the onset of ligninolytic oxidation by *Phanerochaete chrysosporium* on spruce wood. *Appl Environ Microbiol* 81(22):7802–7812.
37. Watanabe T, Tsuda S, Nishimura H, Honda Y, Watanabe T (2010) Characterization of a Δ12-fatty acid desaturase gene from *Ceriporiopsis subvermispora*, a selective lignin-degrading fungus. *Appl Microbiol Biotechnol* 87(1):215–224.
38. Fernandez-Fueyo E, et al. (2012) Comparative genomics of *Ceriporiopsis subvermispora* and *Phanerochaete chrysosporium* provide insight into selective ligninolysis. *Proc Natl Acad Sci USA* 109(14):5458–5463.
39. Yelle DJ, Ralph J, Lu F, Hammel KE (2008) Evidence for cleavage of lignin by a brown rot basidiomycete. *Environ Microbiol* 10(7):1844–1849.
40. Flournoy DS, Kirk TK, Highley TL (1991) Wood decay by brown-rot fungi: Changes in pore structure and cell wall volume. *Holzforschung* 45(5):383–388.
41. Curling SF, Clausen CA, Winandy JE (2002) Relationships between mechanical properties, weight loss, and chemical composition of wood during incipient brown-rot decay. *Forest Products Journal* 52(7):34–39.
42. Mewis K, Lenfant N, Lombard V, Henrissat B (2016) Dividing the large glycoside hydrolase family 43 into subfamilies: A motivation for detailed enzyme characterization. *Appl Environ Microbiol* 82(6):1686–1692.
43. Zhu N, et al. (2016) Comparative analysis of the secretomes of *Schizophyllum commune* and other wood-decay basidiomycetes during solid-state fermentation reveals its unique lignocellulose-degrading enzyme system. *Biotechnol Biofuels* 9:42.
44. Floudas D, et al. (2015) Evolution of novel wood decay mechanisms in *Agaricales* revealed by the genome sequences of *Fistulina hepatica* and *Cylindrobasidium torrendii*. *Fungal Genet Biol* 76:78–92.
45. Thuillier A, et al. (2014) Transcriptomic responses of *Phanerochaete chrysosporium* to oak acetonic extracts: Focus on a new glutathione transferase. *Appl Environ Microbiol* 80(20):6316–6327.
46. Feldman D, Kowbel DJ, Glass NL, Yarden O, Hadar Y (2015) Detoxification of 5-hydroxymethylfurfural by the *Pleurotus ostreatus* lignolytic enzymes aryl alcohol oxidase and dehydrogenase. *Biotechnol Biofuels* 8:63.
47. Gutiérrez A, Caramelo L, Prieto A, Martínez MJ, Martínez AT (1994) Anisaldehyde production and aryl-alcohol oxidase and dehydrogenase activities in ligninolytic fungi of the genus *Pleurotus*. *Appl Environ Microbiol* 60(6):1783–1788.
48. Hernández-Ortega A, Ferreira P, Martínez AT (2012) Fungal aryl-alcohol oxidase: A peroxide-producing flavoenzyme involved in lignin degradation. *Appl Microbiol Biotechnol* 93(4):1395–1410.
49. McQueen-Mason S, Durachko DM, Cosgrove DJ (1992) Two endogenous proteins that induce cell wall extension in plants. *Plant Cell* 4:1425–1433.
50. Quiroz-Castañeda RE, Martínez-Anaya C, Cuervo-Soto LI, Segovia L, Folch-Mallol JL (2011) Loosenin, a novel protein with cellulose-disrupting activity from *Bjerkandera adusta*. *Microb Cell Fact* 10:8.
51. Amadioha AC (1993) A synergism between oxalic acid and polygalacturonases in the depolymerization of potato tuber tissue. *World J Microbiol Biotechnol* 9(5):599–600.
52. Green F, 3rd, Clausen CA, Kuster TA, Highley TL (1995) Induction of polygalacturonase and the formation of oxalic acid by pectin in brown-rot fungi. *World J Microbiol Biotechnol* 11(5):519–524.
53. Schilling JS, Duncan SM, Presley GN, Jurgens JA, Blanchette RA (2013) Colocalizing incipient reactions in wood degraded by the brown rot fungus *Postia placenta*. *Int Biodeterior Biodegradation* 83:56–62.
54. Ghose TK (1987) Measurement of cellulase activities. *Pure Appl Chem* 59(2):257–268.
55. Zhang J, et al. (2012) Improved biomass saccharification by *Trichoderma reesei* through heterologous expression of lacA gene from *Trametes* sp. AH28-2. *J Biosci Bioeng* 113(6):697–703.
56. Aro N, Ilmén M, Saloheimo A, Penttilä M (2003) ACEI of *Trichoderma reesei* is a repressor of cellulase and xylanase expression. *Appl Environ Microbiol* 69(1):56–65.
57. Levasseur A, Drula E, Lombard V, Coutinho PM, Henrissat B (2013) Expansion of the enzymatic repertoire of the CAZy database to integrate auxiliary redox enzymes. *Biotechnol Biofuels* 6(1):41.
58. Lombard V, Golaconda Ramulu H, Drula E, Coutinho PM, Henrissat B (2014) The carbohydrate-active enzymes database (CAZy) in 2013. *Nucleic Acids Res* 42(Database issue, D1):D490–D495.
59. Trapnell C, et al. (2012) Differential gene and transcript expression analysis of RNA-seq experiments with TopHat and Cufflinks. *Nat Protoc* 7(3):562–578.
60. Salame TM, Knop D, Levinson D, Yarden O, Hadar Y (2013) Redundancy among manganese peroxidases in Pleurotus ostreatus. *Appl Environ Microbiol* 79(7):2405–2415.
61. Renart J, Reiser J, Stark GR (1979) Transfer of proteins from gels to diazobenzyloxymethyl-paper and detection with antisera: A method for studying antibody specificity and antigen structure. *Proc Natl Acad Sci USA* 76(7):3116–3120.
62. Song ZW, Vailc A, Sadowsky MJ, Schilling JS (2014) Quantitative PCR for measuring biomass of decomposer fungi in planta. *Fungal Ecol* 7(1):39–46.